Journal of Organometallic Chemistry 695 (2010) 2251–2257

Contents lists available at ScienceDirect

Journal of Organometallic Chemistry

journal homepage: www.elsevier.com/locate/jorganchem

Redox-switchable second-order nonlinear optical responses of TEMPO-dithiolate ligand and (tempodt)M complexes (M = Pt, Pd)

Hai-Bo Zhao, Yong-Qing Qiu*, Chun-Guang Liu, Shi-Ling Sun, Yan Liu, Rong-Shun Wang

Institute of Functional Material Chemistry, Faculty of Chemistry, Northeast Normal University, Changchun 130024, People's Republic of China

ARTICLE INFO

Article history:
Received 30 March 2010
Received in revised form
28 May 2010
Accepted 15 June 2010
Available online 19 June 2010

Keywords:
DFT
Nonlinear optical coefficients
TEMPO
Switchable

ABSTRACT

Density functional theory (DFT) combined with the finite field (FF) method has been carried out to investigate the switching nonlinear optical (NLO) action of the TEMPO-bound dithiolate ligands and metal (Pt, Pd) complexes. The TEMPO unit is a redox-active radical and can stably exist in different redox states (TEMPOH, $TEMPO^+$, TEMPO•, $TEMPO^-$). The DFT–FF calculations show that a substantial enhancement in second-order polarizability has been obtained in $TEMPO^+$-bound dithiolate ligand, with a value of 461×10^{-30} esu. It is because that the TEMPO moiety as donor strength has been lowered by one-electron-reduced, and then the TEMPO moiety becomes the acceptor character in one-electron-oxidized species $^1\mathbf{L}^+$. On the whole, the β_{tot} values of metal complexes within their four different states exhibit excellent NLO switching characters. Thus, this kind of metal complexes has a possibility to be excellent switching second-order NLO materials. Among four states of the metal complexes, the radical **PtL**• and hydroxylamine **PtLH** species are nonlinearity "on", while the one-electron-oxidized $^3\mathbf{PtL}^+$ and one-electron-reduced $^3\mathbf{PtL}^-$ species are nonlinearity "off". It can be seen from the following the real process. Specifically, the electron-acceptor ability of the diimine ligand decreases within its reduction process. However, the electronic character of dithiolate ligand will be changed from electron-donor to electron-acceptor when it is oxidated.

1. Introduction

Multiproperty molecular materials are of growing interest, especially because they should provide opportunities for interplays between the properties, in relation to the emerging concept of molecular switches [1–5]. "Switchable" molecular properties are also of intense interest for sensor applications. Despite this interest, molecules that can stably exist in more than two and independently addressable states, which could be employed for complex and higher-order logic functions, have been explored significantly less than two-state molecules. One potentially important procedure to exploit molecular switches is to utilize their NLO properties [6–9], and in particular their nonlinear absorption. Recently, Green and co-workers show that a specific binuclear metal alkynyl complex incorporating a functionalized 5,5′-dithienylperfluorocyclopentene (DTE) bridge can afford six stable and switchable states at most that possess distinct cubic NLO properties [10]. A more appealing method of controlling the second-order NLO response of a molecule would be a reversible redox change, in which either the donor (D) unit is oxidized or the acceptor (A) unit is reduced [11,12]. The result in either case would be a loss of the charge transfer capability and a consequent drop in the second-order polarizability β. To date, there are many examples in the literature [13–17], one is from the group of Coe, comprising a $\{Ru(NH_3)_5\}^{2+}$ donor linked to a viologen-like acceptor; the value of β decreased by an order of magnitude in one-electron-oxidized process of the Ru(II) center. Subsequent re-reduction of the Ru(II) center completely restored the SHG properties of the complex [18].

Radical and open-shell metal complexes presenting large NLO properties have been actively studied both theoretically and experimentally [19–24]. TEMPO (2, 2, 6, 6- tetramethylpiperidine-1-oxy radical) which as donor in tempodt ligand shows interesting properties attributable to the unpaired electron, and has been extensively employed in preparing functional materials [25,26]. It is well known that the TEMPO radical can participate in various redox reactions and form the reversible systems [27–34] (TEMPOH, $TEMPO^+$, TEMPO•, $TEMPO^-$) (see Chart 1). Despite the wide electrochemical applications of TEMPO and its redox partners, there have been no measurements of the NLO properties for the electron transfer steps linking TEMPO to the reversible redox systems.

* Corresponding author.
E-mail address: qiuyq466@nenu.edu.cn (Y.-Q. Qiu).

0022-328X/$ – see front matter © 2010 Elsevier B.V. All rights reserved.
doi:10.1016/j.jorganchem.2010.06.014

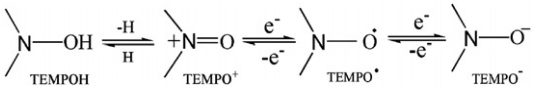

Chart 1. The charge/discharge process of TEMPO radicals.

Especially, the excellent redox properties of the TEMPO moiety can affect the frontier molecular orbitals delocalization, which might cause the change in its NLO properties, thus provide an ideal model for redox switching of NLO responses.

A series of Pt(diimine)(dithiolate) complexes show interesting optical properties, including luminescence and nonlinear optics [35–40]. Scott D. Cummings and co-workers had prepared a series of mixed-ligand transition metal diimine dithiolate complexes, and investigated their nonlinear optical properties. The molecular hyperpolarizabilities of these complexes had been obtained from electric field induced second harmonic generation (EFISHG) experiments at 1.9 μm and range in magnitude from 0 to -39×10^{-30} esu [41]. The direct combination of TEMPO radical and Pt(diimine)(dithiolate) unit into the same molecular system has been achieved by Tetsuro Kusamoto and co-workers [42] recently. Cyclic voltammetry of (tempodt)Pt showed that the first oxidation peak potential (E_p^{ox}) was −0.26 V vs Fc/Fc^+ and the first reduction potentials (E^{red}) was −1.80 V vs Fc/Fc^+. Experimental results showed that the electron absorption spectra of (tempodt)Pt and its one-electron-oxidized species are obviously different from one another. In terms of the sum-over-states (SOS) description of the optical nonlinearity, any modification of the absorption spectrum of a molecule contributes to the modification of the second-order polarizability.

To elucidate the detailed band assignments of the electron spectrum of TEMPO-bound dithiolate ligand (=tempodt) and its Pt complex, the relationship between second-order NLO properties and the molecular structure, and the four stable states switching of the NLO responses in detail, we decided to investigate the four redox states of the tempodt ligands and their metal complexes, where transition metal ions, Pt^{2+} and Pd^{2+}, have been introduced for optimization of the second-order NLO properties (see Fig. 1). The four states are interconvered along such pathway that tempodt **L•** can be reversibly reduced to the $\mathbf{L}^-$, reversibly oxidized to the $\mathbf{L}^+$, and then $\mathbf{L}^+$ is reduced to the hydroxylamine **LH** as depicted in Fig. 1.

2. Computational details

The geometries of all complexes were optimized at the B3LYP (UB3LYP)/6-31G* level. Considering relativistic effects for transition metal ions, the SDD basis set containing the Stuttgart/Dresden effective core potentials [43] was applied for the metal atom. To obtain a more intuitive description of the band assignments of the electron spectrum and the trends in the NLO behavior of the studied complexes, time-dependent density functional theory (TDDFT) method was used to describe the molecular electronic spectra. TDDFT has been used to study the electron spectra of numerous systems, including closed- and open-shell systems. By far, the accuracy and reliability of spin-unrestricted TDDFT for open-shell systems has been tested by studying both the organic and transition metal complexes [44–52]. The present spin-unrestricted calculation shows that the $\langle S^2 \rangle$ of **L•** is 0.753 and these of $\mathbf{L}^-$, $\mathbf{PtL}^+$, $\mathbf{PdL}^+$, $\mathbf{PtL}^-$, $\mathbf{PdL}^-$ are 2.01, 2.03, 2.03, 2.04, 2.03 respectively, which are closed to the theoretical values ($S^2 = 0.75, 2.00$). This indicates that the spin contamination is negligible.

The finite field (FF) method was broadly applied because this methodology can be used in concert with the electronic structure method to compute nonlinear optical coefficients [53]. When a molecule is subjected to a static electric field (F), the energy (E) of the molecule is expressed by eq (1):

$$E = E^{(0)} - \mu_i F_i - \frac{1}{2}\alpha_{ij}F_iF_j - \frac{1}{6}\beta_{ijk}F_iF_jF_k - \frac{1}{24}\gamma_{ijkl}F_iF_jF_kF_l - \cdots\cdots \quad (1)$$

In this expression, $E^{(0)}$ is the energy of the molecule in the absence of an electronic field, μ_i represents the components of the dipole moment vector, α is the linear polarizability tensor, and β and γ are second-order and third-order polarizability tensors, respectively. The subscripts *i, j*, and *k* label *x, y*, and *z* components. The molecular Hamiltonian includes a term ($-\boldsymbol{\mu}\cdot\boldsymbol{F}$) describing the interaction between the external uniformstatic field and the molecule. It is clear that the values of μ, α, β, and γ can be obtained by differentiating E with respect to F. In the present paper, the second-order polarizability β was calculated using the FF method with a field frequency of 0.0010 au at the B3LYP and BHandHLYP two methods in order to get the reliable qualitative analysis. To calculate the dipole moment and the nonlinear optical coefficients tensors, the origin of the Cartesian coordinate system was located at the metal (see Fig. 1). That is, *z*-axe pointed to the TEMPO moiety, the *xz* plane is the plane of molecular. All of the calculations in this work were carried out by using the Gaussian 03 program package [54].

3. Results and discussion

3.1. Redox properties

According to an excess of α-electrons with respect to β-electrons, it therefore can form various spin configurations for tempodt radical in redox processes from the standpoint of theory. Changes of the electronic properties are related to the occupied orbitals, and they also affect the lowest unoccupied orbitals, thus the redox properties of these complexes are changed. Since tempodt and (tempodt)Pt have different redox centers [42], the assignments of the oxidation center, the reduction center and spin states are particularly important. We first determine the stable state and the

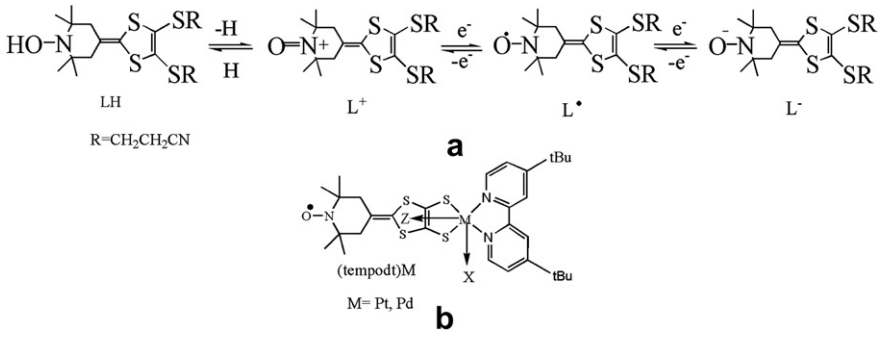

Fig. 1. Structures formula of **LH**, $\mathbf{L}^+$, **L•**, $\mathbf{L}^-$, and (tempodt)M complexes. (M = Pt, Pd).

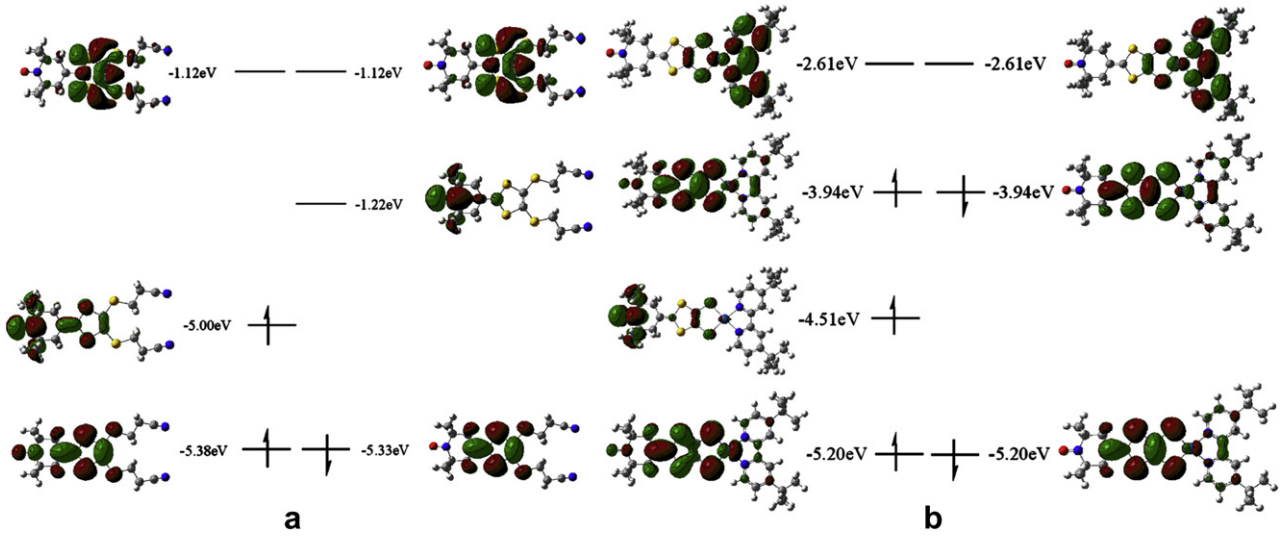

Fig. 2. The molecular orbitals and energy levels of tempodt (a) and (tempodt)Pt (b).

redox center during the four states switching by analyzing the MOs and energy levels of tempodt. As shown in Fig. 2(a), for one-electron-oxidized of tempodt, an electron would be removed from α-HOMO, and then it becomes single state for $^1\mathbf{L}^+$. While for one-electron-reduced of tempodt, an electron would be injected in β-LUMO, the energy of β-LUMO is higher than that of α-HOMO, then it becomes triple state for $^3\mathbf{L}^-$. Both the α-HOMO and the β-LUMO are localized on the TEMPO moiety, it is more likely that the TEMPO unit is the redox center. Unrestricted optimized calculations of one-electron-oxidized and one-electron-reduced species on various spin configurations were performed to check predictions made by molecular orbital analysis. The calculation results also show the energy of the singlet state ($^1\mathbf{L}^+$) lies below that of the triplet state ($^3\mathbf{L}^+$), the triplet state ($^3\mathbf{L}^-$) is more stable than the singlet state ($^1\mathbf{L}^-$). As shown in Fig. 3(a), the spin density of $^3\mathbf{L}^-$ mainly localizes on the TEMPO moiety and dithiolate-base, which is in agreement with the molecular orbital predictions. To further interpret the bonding character of N–O during the redox processes, we performed NBO calculations on ligands. The calculated N–O bond length in the **L•** was 1.289 Å reproducible with 0.01 Å compared to data available in experiment (1.293 Å) and similar to that in other TEMPO derivatives give reliability to our contribution. Table 1 lists selected N–O bond distances, natural bond orbitals, occupancy, orbital coefficients and hybrids, and the orbital types of ligands. The N–O bond distance of $^3\mathbf{L}^-$ (the one-electron-reduced) is similar to that of **L•**. When **L•** is oxidized to the $^1\mathbf{L}^+$ (the one-electron-oxidized), the N–O bond distance decreases and becomes double bond. NBO analysis reveals that N=O double bond of $^1\mathbf{L}^+$ is composed of one N–O σ bond and one N–O π bond, and the σ bond is formed by one N $sp^{2.78}$ orbital and one O $sp^{2.63}$ orbital, while the π bond is made up of one pure p-N orbital and one pure p-O orbital, respectively. **LH** is formed by reducing $^1\mathbf{L}^+$ to the hydroxylamine. Then, the N–O bond distance increases to 1.450 Å. These bond parameters indicate that the N–O site in the TEMPO moiety is the redox center for ligands.

While for the complexes, experimental results indicated that the N–O radical survives under $1e^-$ oxidation of **PtL•**, the peak resulting from the N–O radical bond stretching mode does not appear at around 1650–1700 cm^{-1}, while N=O^+ stretching mode is expected in this range, suggesting that N–O radical is not oxidized [42]. The calculated results show that all stable state metal complexes possess N–O single-bond character, indicating that the redox center is not the TEMPO moiety, but the metal, dithiolate, and diimine. The MOs and energy levels of (tempodt)Pt are shown in Fig. 2(b). The single occupied orbital (SOMO) of **PtL•** is centered on the TEMPO moiety, and the energy level is lower than that of the HOMO, namely the SOMO-HOMO level conversion, triggered by the metal coordination, this result strongly suggests that the removed one electron in the one-electron-oxidized process comes from the HOMO but not from the SOMO. HOMO is composed mainly of sulfur $3p_x$ orbitals that antibonding coaction with metal d_{yz} orbitals and carbon $2p_x$ orbitals contraction on the π-conjugated bridge. The high contribution of sulfur $3p_x$ orbitals on the HOMO orbital is probably the reason that these complexes are easily oxidized to give sulfinated as has been reported before, and it is more likely that the dithiolate-base is the oxidation center. The LUMO orbital is calculated to be almost exclusively located on diimine, it is more likely that diimine ligand accepts the electron in the reduction of **PtL•** to **PtL**$^-$. The drastic electronic structure conversion [42] causes that the triple state is the stable state for one-electron-oxidized species (**PtL**$^+$, **PdL**$^+$) and one-electron-reduced species (**PtL**$^-$, **PdL**$^-$) which are consistent with our computational results. The spin density plots of **PtL•**, ^{3}**PtL**$^+$ and ^{3}**PtL**$^-$ based on the DFT optimized calculations were performed to

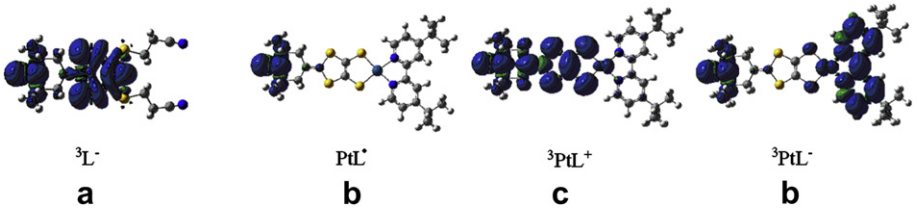

Fig. 3. The spin density plots of $^3\mathbf{L}^-$ (a) and **PtL•**, ^{3}**PtL**$^+$, ^{3}**PtL**$^-$ (b) obtained by UB3LYP/6-31g(d) calculations (SDD basis set on metal ion).

Table 1
The selected natural bond orbitals, bond distances (Å), occupancy, orbital coefficients and hybrids, and orbital type of **L•**, **LH**, ^{3}**L**$^-$, ^{1}**L**$^+$.

Complex	Natural bond orbitals	Bond length (Å)	Occupancy	Orbital coefficients and hybrids	Orbital type
L•	N–O	1.289	0.996	$0.690(sp^{2.92})_N + 0.724(sp^{3.34})_O$	σ
LH	N–O	1.450	1.989	$0.654(sp^{4.47})_N + 0.756(sp^{4.16})_O$	σ
^{3}L$^-$	N–O	1.293	0.996	$0.688(sp^{2.97})_N + 0.725(sp^{3.31})_O$	σ
^{1}L$^+$	N=O	1.224	1.993	$0.683(sp^{2.78})_N + 0.730(sp^{2.63})_O$	σ
			1.990	$0.685(p)_N + 0.729\ (p)_O$	π

Table 2
TDDFT results for the (tempodt)Pt and (tempodt)Pt$^+$ obtained by B3LYP/6-31g(d) calculations (SDD basis set on metal ion).

Complexes	E_{exp}(nm)	E_{calc}(nm)	f_{os}	Major contributions
(tempodt)Pt	650	636	0.0034	α-HOMO → αLUMO + 1(42%) β-HOMO → β-LUMO + 1(55%)
(tempodt)Pt$^+$	820	816	0.2790	β-HOMO − 1 → β-LUMO(97%)
	580	621	0.0277	α-HOMO − 1 → αLUMO(96%)

check predictions made by molecular orbital analysis. It can be seen from Fig. 3(b) that the spin density of **PtL•** mainly localizes on the N–O site in the TEMPO moiety. For one-electron-oxidized species (^{3}**PtL**$^+$) and one-electron-reduced species (^{3}**PtL**$^-$), except for the TEMPO moiety, the spin density also mainly localizes on the π-conjugated dithiolate-base and diimine moiety respectively. The spin density plots show that the redox centers are in agreement with the molecular orbital predictions. The Pd complexes have the same characteristic as Pt complexes. The calculated results show that the one-electron-reduced and -oxidized species must involve orbitals which display predominantly ligands character because the spin densities are nearly independent of the nature of the dithiolate and diimine ligands. These are in agreement with the specific structure of Pt(diimine)(dithiolate) complex. The specific structure is dominated by the existence of the two different unsaturated chelating ligands in the same molecule, one of which is more easily reduced (the diimine ligand) and the other is more easily oxidized (the dithiolate ligand) [55,56].

UV–vis spectra of (tempodt)Pt showed a broad peak around 650 nm, and the peak can be assigned to the intramolecular charge transfer from dithiolate to diimine. In the course of the oxidation of (tempodt)Pt, new peaks at 820 and 940 nm were observed, then the peaks showed a decrease and a new peak at 580 nm was observed as the reaction proceeded [42]. To rationalize the observed spectral properties, the electron absorption spectrum have been calculated in the Gaussian 03 program package at the TD-B3LYP/6-31 G* level. As shown in Table 2, the TDDFT calculations predict that the absorption of (tempodt)Pt at 636 nm can be assigned to ligand-to-ligand charge transfer(LLCT) transition from the β-HOMO to β-LUMO + 1, and the absorption of (tempodt)Pt$^+$ at 816 nm is categorized as intraligand charge transfer (ILCT) combined with metal-to-ligand charge transfer (MLCT) transitions from the β-HOMO − 1 to β-LUMO. The experimental UV–vis spectra results are well reproduced by our DFT and TDDFT calculations.

3.2. Second-order polarizability (β)

The second-order polarizability, β_{tot} for all complexes can be calculated using the following equation:

$$\beta_{tot} = \sqrt{\beta_x + \beta_y + \beta_z} \tag{2}$$

Where β_i is defined by the following formula (3):

$$\beta_i = \beta_{iii} + \frac{1}{3}\sum_{i\neq j}\left[(\beta_{ijj} + \beta_{jij} + \beta_{jji})\right] \quad i,j = x,y,z \tag{3}$$

The ligands and complexes belong to C_{2v} symmetry (**LH**, **PtLH**, **PdLH** belong to C_s), so several β tensor components values are zero. In Table 3, we present the components of β and β_{tot} values of all ligands and complexes with two methods. The calculated results show that β_{xxz}, β_{yyz}, and β_{zzz} are the dominant contributors to the second-order nonlinear optical response. For both ligands and complexes, the β_{tot} values obtained by B3LYP method are larger than those obtained by BHandHLYP method except for **L•**, ^{3}**L**$^+$, but they are basically in the same magnitude. As previous reported, the B3LYP method overestimates the β_{tot} values for some large systems, while BHandHLYP method includes more percentages of HF exchange compared with the B3LYP, then it successfully reduces the overestimation of the second-order polarizability [57–60]. As a result, the β_{tot} values in this paper are based on the BHandHLYP method.

3.2.1. Redox switching of NLO responses for ligands

We investigated the redox center in TEMPO moiety within the four states of the ligands to afford the possibility of NLO switching. In our case, the TEMPO moiety was integrated in the donor part of

Table 3
The second-order polarizabilities (1×10^{-30} esu) obtained by B3LYP and BHandHLYP methods and dipole moments (Debye) of present investigated complexes.

Complex	β_{xxz}		β_{yyz}		β_{zzz}		β_{tot}		μ
	BHandHLYP	B3LYP	BHandHLYP	B3LYP	BHandHLYP	B3LYP	BHandHLYP	B3LYP	B3LYP
L•	−0.50	−0.52	0.13	0.11	−1.15	0.20	1.52	0.22	2.11
LH	−0.41	−0.35	0.09	0.07	0.06	4.45	0.25	4.20	5.70
^{3}L$^-$	2.68	8.07	0.03	0.00	5.80	12.22	8.52	20.29	35.61
^{1}L$^+$	−2.17	−1.60	0.29	0.52	−459.59	−216.09	461.46	217.16	16.12
PtL•	−10.48	−26.06	−1.00	0.75	−210.99	−612.63	222.82	637.94	16.99
PtLH	−11.48	−27.65	−0.97	0.83	−233.80	−754.44	246.25	781.26	14.73
^{3}PtL$^-$	−4.17	−6.72	−1.84	−1.81	−11.15	−25.99	17.16	34.51	11.36
^{3}PtL$^+$	0.09	−4.23	−1.32	−1.18	−71.41	−100.45	72.64	105.87	6.21
PdL•	−6.10	−25.33	−1.81	0.31	−137.12	−742.35	145.03	767.38	17.84
PdLH	−6.52	−27.45	−1.76	0.60	−154.90	−913.38	163.18	940.22	15.61
^{3}PdL$^-$	−5.34	−6.88	−2.10	−2.44	2.38	4.31	5.07	5.01	11.41
^{3}PdL$^+$	1.34	−1.02	−1.60	−154	−5.22	−68.76	52.47	71.32	5.96

Table 4
The oscillator strengths, transition energy, transition moment, and the crucial excited states of ligands.

Complex	f_{os}	E (eV)	M_z^{gm} (a.u.)	Major contributions
$L^{\bullet}$	0.0432	4.3941	0.6332	α HOMO − 1 → α LUMO + 3 (48%) β HOMO − 1 → β-LUMO + 3 (31%)
L^{H}	0.0612	4.0878	0.7819	HOMO − 1 → LUMO + 6 (96%)
	0.0537	4.3622	0.7090	HOMO − 1 → LUMO + 3 (87%)
$^{3}L^{-}$	0.0174	2.0042	0.5944	α-HOMO → α LUMO + 1 (97%)
	0.0181	2.1118	0.5920	βHOMO → β LUMO (99%)
$^{1}L^{+}$	0.1417	0.9528	2.2714	HOMO → LUMO (36%)
	0.1177	4.3719	1.0484	HOMO → LUMO + 2 (80%)

the **L•** on the β_{tot} value. This is known as type I switching [61–63] where the donor ability has been lowered by one-electron-reduced. The β_{tot}value of radical **L•** nearly disappears. While the β_{tot} value of $^{1}\mathbf{L}^{+}$ increases to 461×10^{-30} esu, 303 times as large as that of **L•**. Next $^{1}\mathbf{L}^{+}$ can further reduce to the hydroxylamine **LH**, the β_{tot} value of **LH** also nearly disappears. One-electron-reduced species $^{3}\mathbf{L}^{-}$ shows small increase tendency in β_{tot} value which is 5 times as large as that of **L•**. This indicates that a system corresponds to three forms of nonlinearity "off" in the **L•**, **LH** and $^{3}\mathbf{L}^{-}$ species and one form of nonlinearity "on" in the $^{1}\mathbf{L}^{+}$ species, and thus, this approximation is not well for the second-order NLO switching among four states. However, switching of NLO properties can be achieved between **L•** and one-electron-oxidized species $^{1}\mathbf{L}^{+}$, and potentially, be afforded up to two NLO states. To gain more insight into the redox processes "switching on" optical transition, we have performed TDDFT calculations on electron spectrum (see Table 4). The crucial electron transition (possess a low-energy CT excited state with large oscillator strength) of radical **L•** mainly arises from α-HOMO − 1 to α-LUMO + 3. As shown in Fig. 2(a), α-HOMO − 1 localizes on TEMPO moiety with the π-conjugated dithiolate-base, α-LUMO + 3 localizes on the dithiolate moiety, so TEMPO moiety acts as the donor, dithiolate moiety as the acceptor. In addition, the crucial electron transition character of **LH** is analogous to that of the **L•**, they are all assigned to an ILCT transition. While for the reduced form $^{3}\mathbf{L}^{-}$, the crucial electron transition is from α-HOMO to α-LUMO + 1, α-HOMO localizes on the dithiolate moiety, α-LUMO + 1 localizes on the C≡N acceptor, which is the same as the LLCT from electron-rich dithiolate to classic acceptor C≡N derivatives. For one-electron-oxidized species $^{1}\mathbf{L}^{+}$, the crucial electron transition is from HOMO to LUMO. HOMO localizes on the π-conjugated dithiolate moiety, and minor on N–O site in the TEMPO moiety, however, LUMO localizes on the N–O site in the TEMPO moiety with a minor extension to the π-conjugated dithiolate moiety, which indicates that dithiolate moiety acts as the donor, TEMPO moiety acts as the acceptor. Thus, TEMPO moiety competes with strong C≡N acceptor at the end of ligand, which cause that the direction of charge transfer is altered (see Fig. 4(a)). This LLCT transition is the key factor to originate large NLO response for $^{1}\mathbf{L}^{+}$. The switching effect is illustrated in Fig. 5(a). The characteristics show that TEMPO-centered redox processes influence the intramolecular donor or acceptor character, which accordingly lead to the different nonlinear optical responses.

To further understand the variations in the computed β values, the following two-level expression is employed [64,65]:

$$\beta \propto \frac{\Delta\mu_{gm} f_{gm}}{E_{gm}^{3}} \tag{4}$$

Where f_{gm}, E_{gm} and $\Delta\mu_{gm}$ are the oscillator strength, the transition energy, and the difference of the dipole moment between the ground state (g) and the mth excited state (m), respectively. The second-order polarizabilities are mainly proportional to the oscillator strength and inversely proportional to the cube of the transition energy [66,67]. The transition energies, oscillator strengths, transition moments and the major contributions of crucial excited states [68–71] for ligands are listed in Table 4. The results show that the order of f_{gm}/E_{gm}^{3} values is in agreement with β_{tot} values calculated with FF in either B3LYP method or BHandHLYP method. For $^{1}\mathbf{L}^{+}$, the crucial transition is associated with the lowest transition energy and the highest oscillator strength, so it is reasonable that the β_{tot} value of $^{1}\mathbf{L}^{+}$ is the largest in ligands.

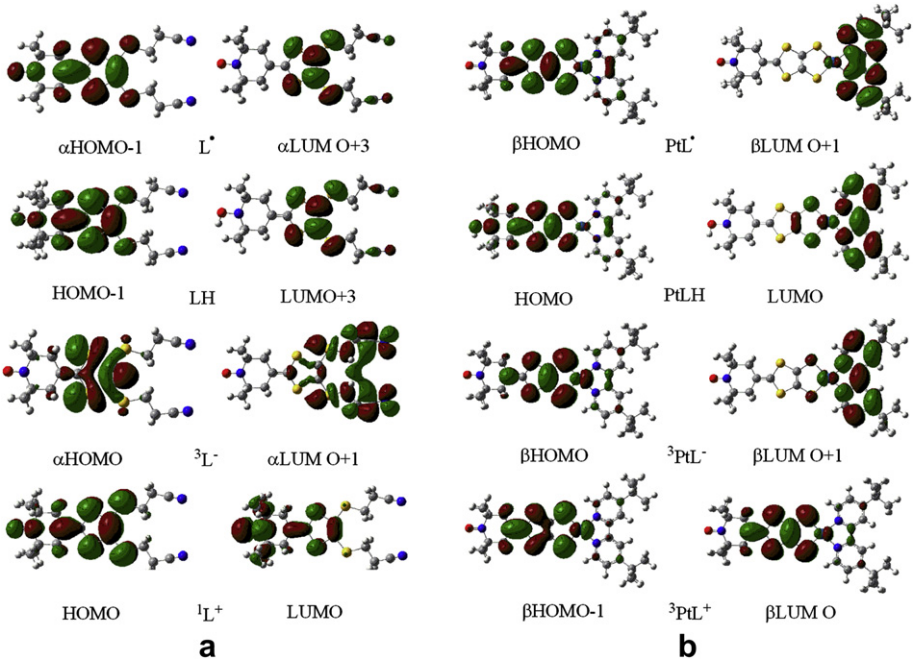

Fig. 4. The orbital transitions associated with the crucial excited states of ligands and complexes obtained by B3LYP/6-31g(d) calculation (SDD basis set on the metal ion).

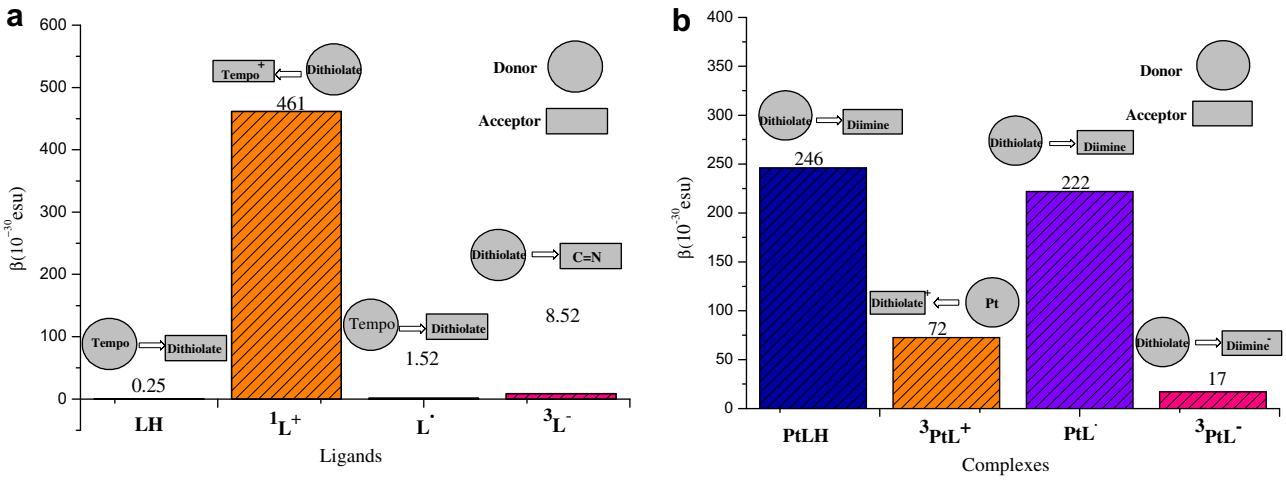

Fig. 5. Comparisons of the first hyperpolarizability of different redox states for ligands (a) and complexes (b) obtained by BHandHLYP/6-31g(d) calculation (SDD basis set on the metal ion).

3.2.2. Redox switching of NLO responses for complexes

Interestingly, the order of β_{tot} values of the Pt complexes is as follows: **PtLH** > **PtL•** > ^{3}**PtL**$^+$ > ^{3}**PtL**$^-$, which reversed the order of β_{tot} values in ligands. On the whole, the β_{tot} values of complexes within their four different states differ largely, suggesting that exchange electron processes are also conducive for the "switching on" the β_{tot} values. The one-electron-reduced and oxidized processes show a decrease in β_{tot} value of ^{3}**PtL**$^-$ and ^{3}**PtL**$^+$. However, **PtL•** and **PtLH** possess considerable large first hyperpolarizabilities, 13 and 14 times as large as that of ^{3}**PtL**$^-$, respectively. **PtL•** and **PtLH** represent a very promising class of complexes for NLO materials, in view of their peculiar electronic structures. This specific structure which is formed by combining an M(II) center with a dithiolate electron-donor ligand and a diimine electron-acceptor ligand leads to a large optical charge transfer. In our case, new dithiolate ligands having electron-donating tempo substituent would be effective in increasing the donor strength of the dithiolate and larger values of β_{tot} than analogues having Rcda, demd, or edt donor ligands substituent [41]. According to the TDDFT calculations, the crucial transition of **PtL•** can be assigned to the β-HOMO → β-LUMO + 1, the intramolecular charge transfer from a π-conjugated dithiolate-based orbital to one that is diimine—based. For **PtLH**, the crucial electron transition is from HOMO to LUMO. As shown in Fig. 4(b), HOMO localizes on the N—O site in the TEMPO with extension to the π-conjugated dithiolate moiety, no pure d_{metal} orbital has been observed due to the noinnocent nature of the dithiolate ligand, while LUMO exhibits the analogous character of the **PtL•** in unoccupied orbitals. The overlap between frontier molecular orbitals is favorable to provide an efficient pathway for ligand-to-metal σ electron donation, thus the ligand-to-ligand charge transfer (LLCT), and substantial ligand-to-metal charge transfer (LMCT), have a biggish contribution to second-order NLO coefficient of **PtLH**. The crucial transitions within ^{3}**PtL**$^-$ have similar character to that of in **PtL•**, which can be assigned to the β-HOMO → β-LUMO + 1. However, the electron-acceptor ability of the diimine ligand has been lowed by one-electron-reduced, which reflects the β_{tot} value decrease. A low-energy π^* orbital of some dithiolates is capable of acting as an acceptor orbital in a charge transfer-to-dithiolate transition. In our case, charge transfer-to-dithiolate excited states have been characterized for ^{3}**PtL**$^+$, molecular orbital calculations suggest that it lies at higher energy than the charge transfer-to-diimine transition. The crucial transitions of ^{3}**PtL**$^+$ are mainly made up of β-HOMO − 1 → β-LUMO. β-HOMO − 1 localizes on the π-conjugated dithiolate moiety and partial on the Pt, while β-LUMO delocalizes over the π-conjugated dithiolate moiety. Two forms of nonlinearity "off" in the ^{3}**PtL**$^-$ and ^{3}**PtL**$^+$ species and two forms of nonlinearity "on" in the **PtL•** and **PtLH** species could become the principal permit switching among four redox states. This situation is illustrated in Fig. 5(b) which depicts the donor/acceptor character in redox processes. The effect of complexes redox processes on the β_{tot} values is opposite, compare to that of the ligands, which indicates that the redox processes can either enhance or decrease the β_{tot} values.

Herein the second-order polarizabilities of (tempodt)Pd analogous complexes are also presented in Table 3. The results indicate that Pt(II) complexes have enhanced β_{tot} values over Pd(II) analogues whose structures differ only in the metal ion. This trend is attributed to the better metal-ligand overlap induced by the 5d-orbitals of Pt compared to 4d-orbitals of Pd, and the higher participation of metal's contribution in occupied (α-HOMO, 22.79% for **PtL•** compared to 18.72% for **PdL•**) and virtual orbitals (α-LUMO, 6.48% for **PtL•** and 4.50% for **PdL•**). The above-mentioned results are agreement with that the greater SHG efficiency of Pt(II) diimine dithiolate complexes relative to Pd(II) diimine dithiolate analogues reported in the literature[41]. The ground-state dipole moment does not change appreciably between complexes with different metal ions, and this result reflects the placement of the metal ion in the center of the molecule, supporting the idea that ground-state dipole moment is insensitive to the metal ion.

4. Conclusions

The TEMPO-bound dithiolate ligands and metal (Pt, Pd) complexes are found to possess a significant potential for reversible switching and modulation of NLO properties by redox process. The results show that for ligands and complexes, they have the different redox centers. Ligands can exist in four stable redox states, and exhibit three forms of nonlinearity "off" in the **L•**, **LH** and ^{3}**L**$^-$ species and one form of nonlinearity "on" in the ^{1}**L**$^+$ species. The DFT—FF calculations indicate that the redox processes significantly affect the TEMPO moiety as donor/acceptor ability and change the charge transfer feature. Thus, the β_{tot} value of one-electron-oxidized species, ^{1}**L**$^+$, increases to 461 × 10^{-30} esu, 303 times as large as that of TEMPO• radical ligand. For complexes, the β_{tot} values of **PtL•** and **PtLH** are large and very close in magnitude of 222 × 10^{-30} esu, 246 × 10^{-30} esu respectively, and this attribute to their specific structure. The specific structure combining of a dithiolate electron-donor ligand which is more easily oxidized

and a diimine electron-acceptor ligand which is more easily reduced, at the same time, the two ligands coordinated to an M(II) center lead to a large charge transfer. The one-electron-reduced and -oxidized of **PtL•** cause a decrease in the β_{tot} values. The two forms of nonlinearity "off" in the ^{3}**PtL**$^{-}$ and ^{3}**PtL**$^{+}$ species and two forms of nonlinearity "on" in the **PtL•** and **PtLH** species could become the principal permit switching between four redox states. By analyzing TDDFT calculations on electron spectrum, the results show that large NLO response is strongly related to the ligand-to-ligand charge transfer (LLCT) transitions. Our investigation has not only turned out the origin of larger NLO values in TEMPO-bound dithiolate ligands and metal (Pt, Pd) complexes but also predicted the possible significant potential of the present studies systems as a new type of "On/Off" switchable NLO molecular materials.

Acknowledgments

The authors gratefully acknowledge the financial support from the National Natural Science Foundation of China (No. 20873017), Program for Chang jiang Scholars and Innovative Research Team in University (IRT0714).

References

[1] M.D. Ward, Chem. Soc. Rev. 24 (1995) 121–134.
[2] C.G. Liu, W. Guan, P. Song, L.K. Yan, Z.M. Su, Inorg. Chem. 48 (2009) 6548–6554.
[3] J.F. Létard, S. Montant, P. Guionneau, P. Martin, A. LeCalvez, E. Freysz, D. Chasseau, R. Lapouyade, O. Kahn, Chem. Commun. 8 (1997) 745–746.
[4] C.G. Liu, Y.Q. Qiu, Z.M. Su, G.C. Yang, S.L. Sun, J. Phys. Chem. C 112 (2008) 7021–7028.
[5] W. Guan, G.C. Yang, C.G. Liu, P. Song, L. Fang, L.K. Yan, Z.M. Su, Inorg. Chem. 47 (2008) 5245–5252.
[6] L.B. Lecaque, B.J. Coe, K. Clays, S. Foerier, T. Verbiest, I. Asselberghs, J. Am. Chem. Soc. 130 (2008) 3286–3287.
[7] I. Asselberghs, K. Clays, A. Persoons, A.M. McDonagh, M.D. Ward, J.A. McCleverty, Chem. Phys. Lett. 368 (2003) 408–411.
[8] J.A. Delaire, K. Nakatani, Chem. Rev. 100 (2000) 1817–1845.
[9] S. Muhammad, M.R.S. A Janjua, Z.M. Su, J. Phys. Chem. C 113 (2009) 12551–12557.
[10] K.A. Green, M.P. Cifuentes, T.C. Corkery, M. Samoc, M.G. Humphrey, Angew. Chem. 48 (2009) 7867–7870.
[11] E. Hendrickx, K. Clays, A. Persoons, C. Dehu, J.L. Bíedas, J. Am. Chem. Soc. 117 (1995) 3547–3555.
[12] R. Loucif-Saïbi, K. Nakatani, J.A. Delaire, M. Dumont, Z. Sekkat, Chem. Mater. 5 (1993) 229–236.
[13] G.T. Dalton, M.P. Cifuentes, S. Petrie, R. Stranger, M.G. Humphrey, M. Samoc, J. Am. Chem. Soc. 129 (2007) 11882–11883.
[14] M.P. Cifuentes, C.E. Powell, M.G. Humphrey, G.A. Heath, M. Samoc, B. Luther-Davies, J. Phys. Chem. A 105 (2001) 9625–9627.
[15] C.E. Powell, M.P. Cifuentes, J.P.L. Morrall, R. Stranger, M.G. Humphrey, M. Samoc, B. Luther-Davies, G.A. Heath, J. Am. Chem. Soc. 125 (2003) 602–610.
[16] C.E. Powell, M.G. Humphrey, M.P. Cifuentes, J.P. Morrall, M. Samoc, B. Luther-Davies, J. Phys. Chem. A 107 (2003) 11264–11266.
[17] M.P. Cifuentes, C.E. Powell, J.P. Morrall, A.M. McDonagh, N.T. Lucas, M. G. Humphrey, M. Samoc, S. Houbrechts, I. Asselberghs, K. Clays, A. Persoons, T. Isoshima, J. Am. Chem. Soc. 128 (2006) 10819–10832.
[18] B.J. Coe, S. Houbrechts, I. Asselberghs, A. Persoons, Angew. Chem. 38 (1999) 366–369.
[19] C.C. Lu, E. Bill, T. Weyhermüller, E. Bothe, K. Wieghardt, J. Am. Chem. Soc. 130 (2008) 3181–3197.
[20] S. Ohta, M. Nakano, T. Kubo, K. Kamada, K. Ohta, R. Kishi, N. Nakagawa, B. Champagne, E. Botek, A. Takebe, S. Umezaki, M. Nate, H. Takahashi, S. Furukawa, Y. Morita, K. Nakasuji, K. Yamaguchi, J. Phys. Chem. A 111 (2007) 3633–3641.
[21] Z.J. Li, F.F. Wang, Z.R. Li, H.L. Xu, X.R. Huang, D. Wu, W. Chen, G.T. Yu, F.L. Gu, Y. Aoki, Phys. Chem. Chem. Phys. 11 (2009) 402–408.
[22] J. Gradinaru, A. Forni, V. Druta, F. Tessore, S. Zecchin, S. Quici, N. Garbalau, Inorg. Chem. 46 (2007) 884–895.
[23] B.J. Coe, J. Fielden, S.P. Foxon, B.S. Brunschwig, I. Asselberghs, K. Clays, A. Samoc, M. Samoc, J. Am. Chem. Soc. 132 (2010) 3496–3513.
[24] B.J. Coe, S.P. Foxon, E.C. Harper, M. Helliwell, J. Raftery, C.A. Swanson, B.S. Brunschwig, K. Clays, E. Franz, J. Garín, J. Orduna, P.N. Horton, M.B. Hursthouse, J. Am. Chem. Soc. 132 (2010) 1706–1723.
[25] K. Mitsudo, T. Kaide, E. Nakamoto, K. Yoshida, H. Tanaka, J. Am. Chem. Soc. 129 (2007) 2246–2247.
[26] Y. Yonekuta, K. Susuki, K. Oyaizu, K. Honda, H. Nishide, J. Am. Chem. Soc. 129 (2007) 14128–14129.
[27] J.R. Fish, S.G. Swarts, M.D. Sevilla, T. Malinski, J. Phys. Chem. 92 (1988) 3745–3751.
[28] K. Nakahara, K. Iwasa, J. Iriyama, Y. Morioka, M. Suguro, M. Satoh, E.J. Cairns, Electrochimi. Acta 52 (2006) 921–927.
[29] A.C. Herath, J.Y. Becker, Electrochimi. Acta 53 (2008) 4324–4330.
[30] I. Cianga, T. Senyo, K. Ito, Y. Yagci, Macromol. Rapid Commun. 25 (2004) 1697–1702.
[31] R.A. Sheldon, I.W.C.E. Arends, J. Mol. Catal. A: Chem. 251 (2006) 200–214.
[32] R.A. Sheldon, I.W.C.E. Arends, Adv. Synth. Catal. 346 (2004) 1051–1071.
[33] X.L. Wang, R. Liu, Y. Jin, X.M. Liang, Chem. Eur. J. 14 (2008) 2679–2685.
[34] J.Q. Qu, F.Z. Khan, M. Satoh, J. Wada, H. Hayashi, K. Mizoguchi, T. Masuda, Polymer 49 (2008) 1490–1496.
[35] W. Paw, S.D. Cummings, M.A. Mansour, W.B. Connick, D.K. Geiger, R. Eisenberg, Coord. Chem. Rev. 171 (1998) 125–150.
[36] K. Base, M.T. Tierney, A. Fort, J. Muller, M.W. Grinstaff, Inorg. Chem. 38 (1999) 287–289.
[37] N.M. Shavaleev, E.S. Davies, H. Adams, J. Best, J.A. Weinstein, Inorg. Chem. 47 (2008) 1532–1547.
[38] J.S. Pap, F.L. Benedito, E. Bothe, E. Bill, S.D. George, T. Weyhermüller, K. Weighardt, Inorg. Chem. 46 (2007) 4187–4196.
[39] T.M. Cocker, R.E. Bachman, Inorg. Chem. 40 (2001) 1550–1556.
[40] E.A.M. Geary, L.J. Yellowlees, L.A. Jack, I.D.H. Oswald, S. Parsons, N. Hirata, J.R. Durrant, N. Robertson, Inorg. Chem. 44 (2005) 242–250.
[41] S.D. Cummings, L.T. Cheng, R. Eisenberg, Chem. Mater. 9 (1997) 440–450.
[42] T. Kusamoto, S. Kume, H. Nishihara, J. Am. Chem. Soc. 130 (2008) 13844–13845.
[43] T.H. . Dunning Jr., P.J. Hay, in: H.F. Schaefer III (Ed.), Modern Theoretical Chemistry, vol. 3, Plenum, New York, 1976, pp. 1–28.
[44] J. Guan, M.E. Casida, D.R. Salahub, J. Mol. Struct. Theochem 527 (2000) 229–244.
[45] B. Champagne, M. Guillaume, F. Zutterman, Chem. Phys. Lett. 425 (2006) 105–109.
[46] G.C. Yang, L. Fang, K. Tan, S.Q. Shi, Z.M. Su, R.S. Wang, Organometallics 26 (2007) 2082–2087.
[47] S. Hirata, M. Head-Gordon, Chem. Phys. Lett. 302 (1999) 375–382.
[48] A. Spielfiedel, N.C. Handy, Phys. Chem. Chem. Phys. 1 (1999) 2401–2409.
[49] C. Adamo, V. Barone, Chem. Phys. Lett. 314 (1999) 152–157.
[50] E. Broclawik, T. Borowski, Chem. Phys. Lett. 339 (2001) 433–437.
[51] B. Dai, K.M. Deng, J.L. Yang, Q.S. Zhu, J. Chem. Phys. 118 (2003) 9608–9613.
[52] V.N. Nemykin, P. Basu, Inorg. Chem. 42 (2003) 4046–4056.
[53] D.R. Kanis, M.A. Ratner, T.J. Marks, Chem. Rev. 94 (1994) 195–242.
[54] M.J. Frisch, G.W. Trucks, H.B. Schlegel, G.E. Scuseria, M.A. Robb, J.R. Cheeseman, J.A. Montgomery Jr., T. Vreven, K.N. Kudin, J.C. Burant, J.M. Millam, S.S. Iyengar, J. Tomasi, V. Barone, B. Mennucci, M. Cossi, G. Scalmani, N. Rega, G.A. Petersson, H. Nakatsuji, M. Hada, M. Ehara, K. Toyota, R. Fukuda, J. Hasegawa, M. Ishida, T. Nakajima, Y. Honda, O. Kitao, H. Nakai, M. Klene, X. Li, J.E. Knox, H.P. Hratchian, J.B. Cross, C. Adamo, J. Jaramillo, R. Gomperts, R.E. Stratmann, O. Yazyev, A.J. Austin, R. Cammi, C. Pomelli, J.W. Ochterski, P.Y. Ayala, K. Morokuma, G.A. Voth, P. Salvador, J.J. Dannenberg, V.G. Zakrzewski, S. Dapprich, A.D. Daniels, M.C. Strain, O. Farkas, D.K. Malick, A.D. Rabuck, K. Raghavachari, J.B. Foresman, J.V. Ortiz, Q. Cui, A.G. Baboul, S. Clifford, J. Cioslowski, B.B. Stefanov, G. Liu, A. Liashenko, P. Piskorz, I. Komaromi, R.L. Martin, D.J. Fox, T. Keith, M.A. Al-Laham, C.Y. Peng, A. Nanayakkara, M. Challacombe, P.M.W. Gill, B. Johnson, W. Chen, M.W. Wong, C. Gonzalez, J.A. Pople, Gaussian 03, Revision C.02. Gaussian, Inc., Wallingford, CT, 2004.
[55] C. Makedonas, C.A. Mitsopoulou, Eur. J. Inorg. Chem. 3 (2006) 590–598.
[56] C. Makedonas, C.A. Mitsopoulou, F.J. Lahoz, A.L. Balana, Inorg. Chem. 42 (2003) 8853–8865.
[57] B. Champagne, E.A. Perpète, D. Jacquenmin, S.J.A. van Gisbergen, E.J. Baerends, C. Soubra-Ghaoui, K.A. Robins, J. Phys. Chem. A 104 (2000) 4755–4763.
[58] B. Champagne, E. Botek, M. Nakano, T. Nitta, K. Yamaguchi, J. Chem. Phys. 122 (2005) 114315–114326.
[59] M. Nakano, R. Kishi, T. Nitta, T. Kubo, J. Phys. Chem. A 109 (2005) 885–891.
[60] Y.Q. Qiu, H.L. Fan, S.L. Sun, C.G. Liu, Z.M. Su, J. Phys. Chem. A 112 (2008) 83–88.
[61] A. Wahab, M. Bhattacharya, S. Ghosh, A.G. Samuelson, P.K. Das, J. Phys. Chem. B. 112 (2008) 2842–2847.
[62] T. Weyland, I. Ledoux, S. Brasselet, J. Zyss, C. Lipinte, Organometallics 19 (2000) 5235–5237.
[63] B.J. Coe, Chem. Eur. J. 5 (1999) 2464–2471.
[64] J.L. Oudar, D.S. Chemla, J. Chem. Phys. 66 (1976) 2664–2668.
[65] J.L. Oudar, J. Chem. Phys. 67 (1977) 446–457.
[66] S.J. Lalama, A.F. Garito, Phys. Rev. A 20 (1979) 1179–1194.
[67] B.F. Levine, C.G. Bethea, J. Chem. Phys. 66 (1977) 1070–1074.
[68] W. Chen, Z.R. Li, D. Wu, Y. Li, C.C. Sun, F.L. Gu, J. Am. Chem. Soc. 127 (2005) 10977–10981.
[69] W. Chen, Z.R. Li, D. Wu, Y. Li, C.C. Sun, F.L. Gu, Y. Aoki, J. Am. Chem. Soc. 128 (2006) 1072–1073.
[70] H.L. Xu, Z.R. Li, D. Wu, B.Q. Wang, Y. Li, F.L. Gu, Y. Aoki, J. Am. Chem. Soc. 129 (2007) 2967–2970.
[71] W. Chen, Z.R. Li, D. Wu, Y. Li, C.C. Sun, F.L. Gu, J. Am. Chem. Soc. 127 (2005) 4845–4859.